PHILOSOPHICAL TRANSACTIONS OF THE ROYAL SOCIETY B BIOLOGICAL SCIENCES

Optical Diffraction Studies of Myofibrillar Structure

E. J. O'Brien, Pauline M. Bennett and Jean Hanson

Phil. Trans. R. Soc. Lond. B 1971 **261**, 201-208
doi: 10.1098/rstb.1971.0051

Phil. Trans. Roy. Soc. Lond. B. **261**, 201–208 (1971) [201]
Printed in Great Britain

Optical diffraction studies of myofibrillar structure

By E. J. O'Brien, Pauline M. Bennett and Jean Hanson, F.R.S.
M.R.C. Biophysics Unit, Department of Biophysics, King's College,
26–29 *Drury Lane, London, W.C.* 2

[Plates 36 to 39]

We have used the techniques of optical diffraction and optical filtering to study electron micrographs of myofibrils and of paracrystals of myofibrillar proteins. The optical diffraction patterns provide information about periodic structure in the micrographs, and sometimes may reveal periodicities not apparent to the eye. We compare the optical diffraction patterns with the X-ray diffraction patterns obtained from living muscle, and this comparison can assist our interpretation of both the X-ray diffraction patterns and the electron micrographs.

The optical diffractometer we have used is essentially similar to those described by Taylor & Lipson (1964), and by Klug & DeRosier (1966). The apparatus incorporates several refinements to facilitate operation. The recombining lens has a focal length, f, of about 1 m, and is placed so that the recombined image is formed at $2f$ and has the same size as the subject. The diffraction subjects are not usually the electron micrographs themselves but copies on film. The film is of more uniform optical thickness than the glass electron micrograph, and is less fragile. Moreover, a set of films of varying contrast can be made from one micrograph.

Actin paracrystals

(*a*) *Introduction*

When F actin is precipitated from solution by magnesium ions, paracrystalline arrays of F actin filaments are formed (Hanson 1967, 1968*b*). A variety of preparations of paracrystals of both pure and impure F actin have been examined (see later for preparative details). The impure actin contains, in particular, the regulatory proteins tropomyosin and 'troponin' (Ebashi & Endo 1968; Ebashi, Endo & Ohtsuki 1969; Schaub & Perry 1969). Pure and impure actin paracrystals might show differences of structure that could be attributed to the presence or absence of the regulatory proteins, and hence throw light on the mechanism regulating the actin–myosin interaction in muscle.

The symmetry of the actin filament is well understood (Selby & Bear 1956; Hanson & Lowy 1963). The filament consists of helically arranged globular subunits with approximately thirteen subunits in six turns of the genetic helix. This arrangement may be regarded as two long-pitch helical chains wound round each other. The distance along the filament axis between successive cross-over points of the two chains, that is, half the pitch length of one chain, is about 36 nm, measured by X-ray diffraction of living, resting muscle (Huxley & Brown 1967; Lowy & Vibert 1967).

(*b*) *Pure actin paracrystals*

Electron micrographs of paracrystals of highly purified actin show that they are parallel arrays of F actin filaments arranged in register with the cross-over points transversely alined. Optical diffraction patterns of these micrographs have intensity distributions consistent with

the presence of helical filaments. Figures 1*a* and 1*b*, plate 36, show a paracrystal and its diffraction pattern. The two strongest layer-lines have axial spacings in the ratio 6.0 ± 0.2. Within the experimental error, they are the first and sixth orders of a repeat of 35 nm, indicating that the helix is integral with 13 subunits in 6 turns. Note that the seventh layer-line, which, like the sixth, has a contribution from the J_1 Bessel term, is very weak. The position of the first row-line in the diffraction pattern indicates that the lateral separation of the filaments is about 6.0 nm, rather small if we consider that the actin subunit may have a diameter of approximately

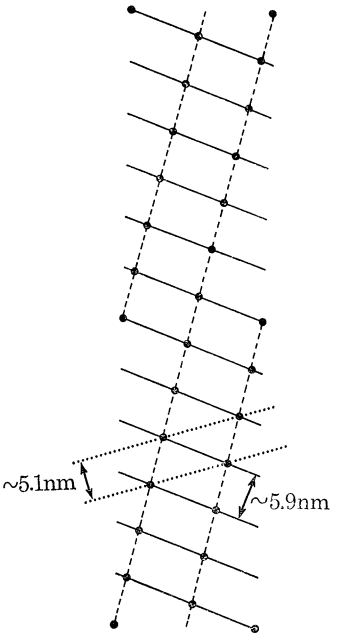

FIGURE 2. The radial projection of a helix with thirteen subunits in six turns. Indexing of the optical diffraction patterns of the electron micrographs of actin paracrystals indicates that the actin filament in the micrographs has integral symmetry of the type shown here. The same symmetry is not necessarily present in living muscle (see Hanson 1967).

5.5 nm (Hanson & Lowy 1963). Such a small separation might have been expected if the filaments had been arranged not with the cross-over points alined but with adjacent filaments translated parallel to the filament axis by half the distance between cross-over points, that is, half of 35 nm. A filament translation would enable the long-pitch helical chain of one filament to interleave with the long-pitch helical groove of the next. This interlocking of 'ridge' and 'groove' is a feature of the close packing of 'smooth' helical filaments, that is, helical filaments which, as a first approximation, lack fine surface detail (Klug & Franklin 1958; Marvin 1958). Molecules with non-integral helical symmetry are likely to pack as smooth helices, since the pattern of contacts between neighbouring molecules varies after every pitch length and is thus non-specific (Marvin, Spencer, Wilkins & Hamilton 1961). Hence the absence of ridge-and-groove packing in the actin paracrystals suggests that the actin filaments have integral symmetry and that there are specific interactions between adjacent filaments. Examination of very many electron micrographs indicates that the paracrystals are two-dimensional, ribbon-like structures. Hence the small filament separation cannot be attributed to the foreshortening effect that would occur if adjacent filaments were lying slightly over each other. The subunits in adjacent filaments must, therefore, interdigitate. This feature can be observed in many electron

micrographs, and is clearly present in the image obtained by optical filtering (figure 1*c*), where the 'noise' spectra present in the diffraction pattern, that is, the diffracted rays that cannot be indexed on the actin lattice, are filtered out. The interdigitation suggests that the actin subunits are not spherical but are somewhat elongated. Asymmetry in the shape of the subunit is also indicated by the very large difference in intensity between the sixth and seventh layer-lines of the diffraction pattern. The difference cannot be explained simply by the fall-off in the transform of a spherical subunit since the eighth layer-line is stronger than the seventh. Figure 2 shows the actin helical net. The planes marked ~ 5.9 nm and ~ 5.1 nm give rise to the sixth and seventh layer-line reflexions. To make the ~ 5.9 nm planes stronger and the ~ 5.1 nm planes weaker the subunits should be elongated along the ~ 5.9 nm planes. This description is oversimplified since the helical net is two-dimensional and the actual structure three-dimensional, but is correct as a first approximation.

(*c*) *Impure actin paracrystals*

Figure 3*a*, plate 36, shows paracrystals formed from impure actin. The filaments appear to be spaced further apart than in the pure actin paracrystals, and this increased spacing is revealed clearly in the diffraction pattern (figure 3*b*) where the first row-line gives a spacing about 20% greater. The axial repeat is not significantly different from the previous value of 35 nm, and the indexing of the layer-lines indicates that the helix has the same or nearly the same symmetry as that of pure actin. The intensity distribution is different, however (cf. figures 1*b* and 3*b*). The first layer-line is now weak where before it was strong, and the second layer-line is strong where before it was weak. (We find this feature in many, though not all, of the diffraction patterns recorded; in the other patterns both reflexions are weak.) This change of relative intensities of the first and second layer-lines would occur if the additional material in the impure paracrystals were situated in the long-pitch helical grooves of the actin filament. In figure 2 the long-pitch helical chains are shown by dashed lines, and the first and second layer-line reflexions correspond to the first and second order reflexions from these lines. The introduction of material along a line midway between the dashed lines would weaken the first-order reflexion and strengthen the second. The 'noise-free' filtered image of the impure paracrystals (figure 3*c*) does not show clearly or directly where the extra material is located, but we must bear in mind that the resolution in this image is limited to about 3.0 nm, probably not sufficient to distinguish between the actin and the extra material. Nevertheless, the image does appear considerably different from its counterpart in figure 1*c*. The cross-over points of the long-pitch helical chains are less well marked, and appear to occur at half the previous value of 35 nm, that is, at one quarter of the actin helical repeat (70 nm). Extra material in the long-pitch grooves could produce, at low resolution, an apparent halving of the distance between cross-over points. Although the filtered image does not show this halving clearly, we would nevertheless *expect* to observe a feature at 17.5 nm since the second layer-line in the diffraction pattern is stronger than the first.

The diffraction pattern in figure 3*b* shows row-lines spaced at 1/7 nm^{-1}. The positions of these are clearly marked by the maxima along the equator. There are additional, weaker row-lines located midway between the main ones. The position of the first additional row-line is indicated on the sixth and seventh layer-lines, between the meridian and the first main row-line. The second additional row-line can be seen on the first and second layer-lines, between the first and second main row-lines. The presence of these intermediate row-lines is very well

PHILOSOPHICAL TRANSACTIONS OF THE ROYAL SOCIETY B BIOLOGICAL SCIENCES

marked on some of the diffraction patterns we have recorded, particularly on those obtained from paracrystals with a larger number (6 to 10) of filaments. There is little sign of intermediate row-lines in the diffraction patterns obtained from pure actin paracrystals. We infer that in the impure paracrystals the filaments are grouped in pairs, so that the true crystallographic repeat in the direction perpendicular to the filament axis is 2×7 nm. The filtered image in figure 3*c* indicates that successive filaments are 'staggered', each filament being translated parallel to the filament axis direction by one-eighth of the actin helical repeat, that is, by 70/8 nm. This one-eighth translation would be expected for an assembly of *four*-stranded helical filaments arranged with ridge-and-groove packing. Hence the impure filaments, that is, F actin with extra material in the long-pitch helical grooves, appear to behave as four-stranded, smooth helices. This is a preliminary result, and further work is needed to clarify the nature and significance of the filament packing in the impure paracrystals.

Impure actin paracrystals often appear striped (figure 4, plate 39). The stripes can be seen more easily where the paracrystals are folded and provide better contrast, but can also be seen in the flat paracrystals, as in figure 3*a*. The filtered image in figure 3*c* shows regions of greater contrast where the stripe material is located, but the relation between the stripe material and the mode of packing discussed in the last paragraph is obscure. Evidence from other work (J. Hanson, unpublished) indicates that the stripes are due to the presence of troponin.

Our observations are in general agreement both with the model proposed by Hanson & Lowy (1963), in which tropomyosin lies in the long-pitch helical grooves of the actin filament, and with the model of Ebashi *et al.* (1969) in which troponin molecules adhere to the actin–tropomyosin complex at intervals of about 40 nm.

Muscle sections

Figure 5, plate 37, shows an electron micrograph, provided by Dr Sally Page, of a longitudinal section of frog sartorius muscle. Running perpendicular to the filaments in the I and A bands of the sarcomere there is a series of fine striations. The striations are well defined in the I band, but those in the A band, both in the H zone and in the region where the thin and thick filaments overlap, generally appear confused. The I band striations have a periodicity of 38.2 ± 1.0 nm, measured on this micrograph by Dr Page. The method of specimen preparation minimized shrinkage in the filaments.

Figure 6*a*, plate 37, shows an optical diffraction pattern obtained from the whole area of the section shown in figure 5. Figure 6*b* is a pattern from a smaller area, and is less intense. The patterns show equatorial reflexions arising from the lateral spacing of the filaments. In addition, there are a number of meridional reflexions, one of which is particularly strong. Using the micrograph magnification determined by Dr Page, we measure from the strong reflexion a spacing of 38.5 nm. We can easily tell that this spot derives from the I band by masking off all except the I bands before recording the diffraction pattern. *All* the other prominent meridional reflexions are observed in diffraction patterns obtained from the H zones alone and hence arise from the thick filament assembly. They have spacings of 50, 44.5, 27, 18.5 and 14.5 nm. These spacings and also the 38.5 nm spacing are the same in micrographs of both long and short sarcomeres, thus confirming that differential shrinkage of the filaments during specimen preparation was negligible.

PHILOSOPHICAL TRANSACTIONS OF THE ROYAL SOCIETY B BIOLOGICAL SCIENCES

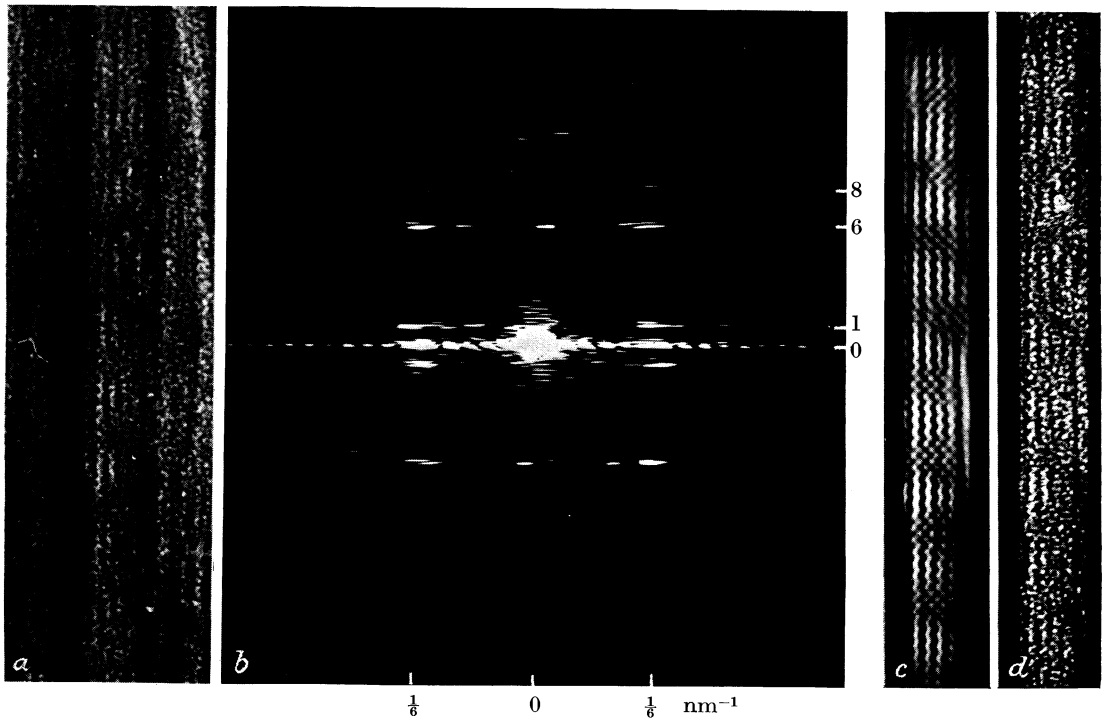

FIGURE 1. (*a*) A paracrystal of highly purified actin, negatively stained with 1% uranyl acetate. (*b*) Optical diffraction pattern of part of (*a*). (*c*) Filtered image of part of (*a*). The filter masked out all but the strong diffracted rays and hence excluded the 'noise' spectra, that is, the diffracted rays that could not be indexed on the actin lattice. (*d*) The image of the same part of (*a*) recorded by the apparatus without a filter. (Magnification of (*a*), (*c*) and (*d*) ×270 000.) The protein is white in (*a*), (*c*) and (*d*).

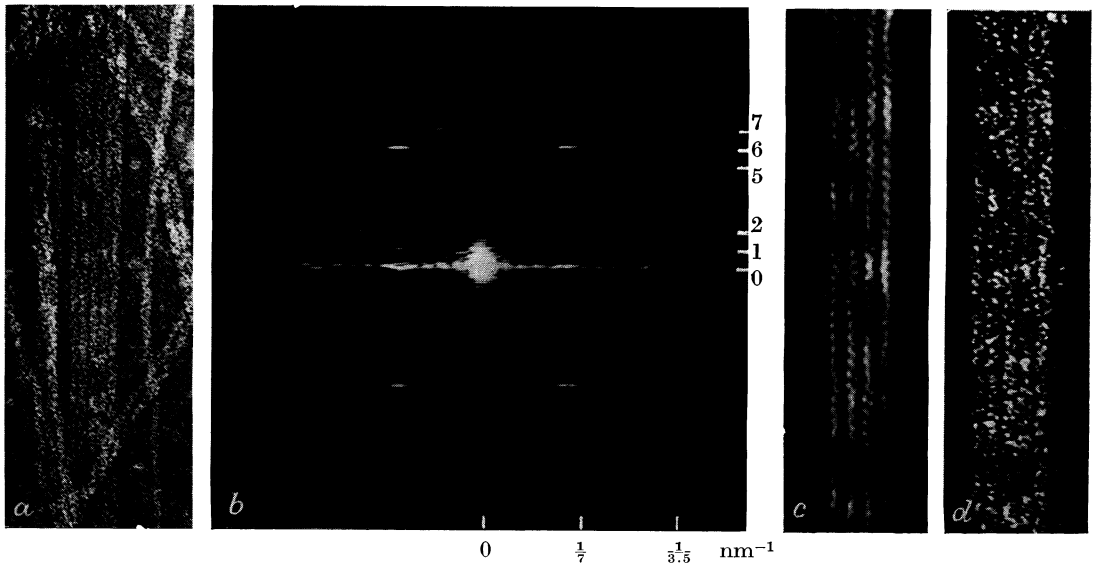

FIGURE 3. (*a*) to (*d*) The sequence of figure 1 repeated for an impure actin paracrystal (pure actin plus impure tropomyosin). The preparation was fixed with glutaraldehyde and negatively stained with 1% uranyl acetate. The optical diffraction pattern differs from that in figure 1 chiefly in the change of row-line spacing, reversal of relative intensities of the first and second layer-lines, and introduction of weak row-lines midway between the main ones. In the filtered image, the cross-over points may be seen more clearly near the centre of the photograph, especially when it is viewed obliquely along its length. (Magnification of (*a*) ×160 000, (*c*) and (*d*) ×270 000.)

(*Facing p.* 204)

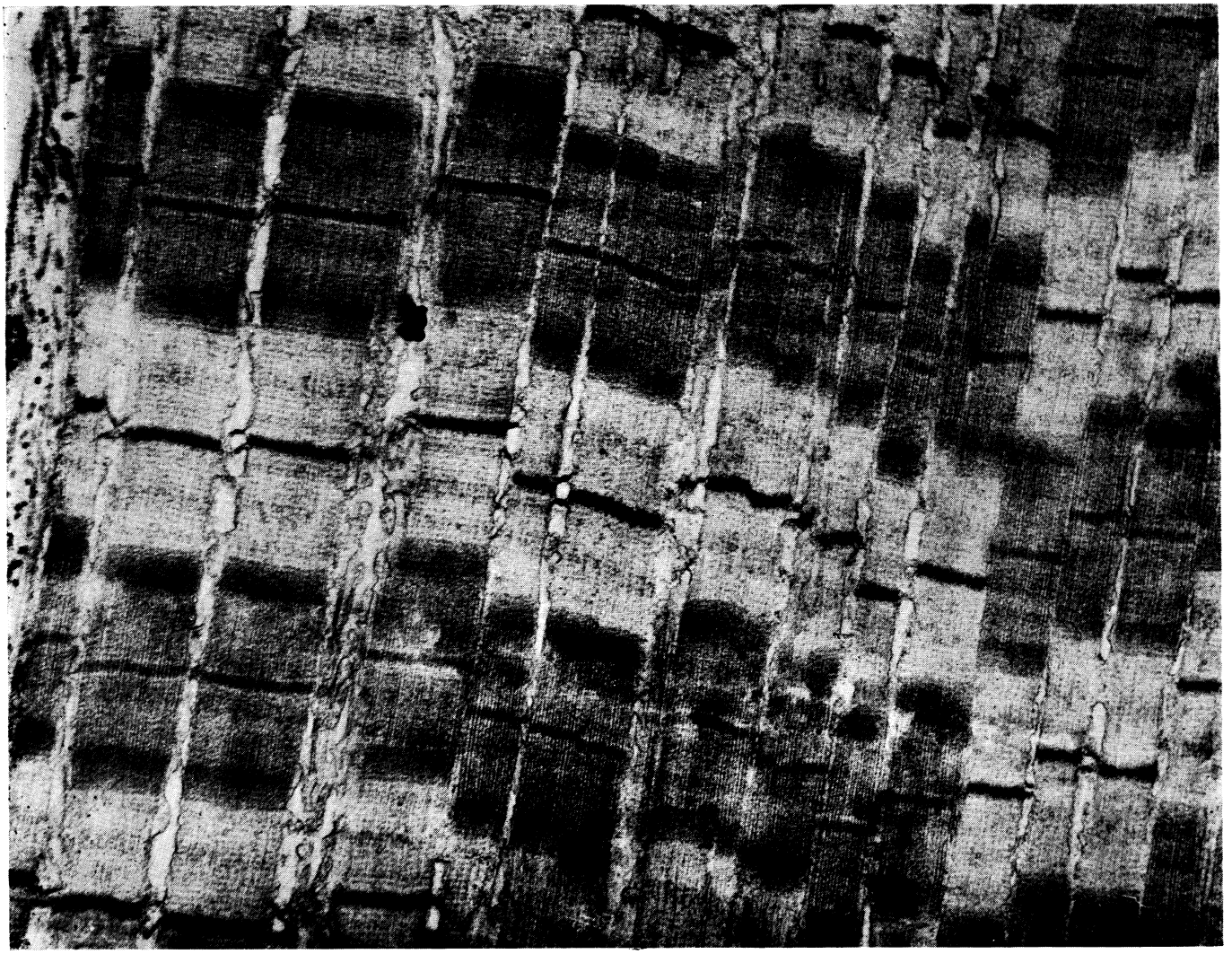

FIGURE 5. Longitudinal section of frog sartorius muscle, positively stained with phosphotungstic acid. The muscle was clamped at either end during fixation with OsO_4 and dehydration with ethanol, and was electrically stimulated during fixation. Changes of filament length were thus minimized (Page 1964; Page & Huxley 1963). The section was cut with the knife edge parallel to the fibre axis (magn. ×24 000).

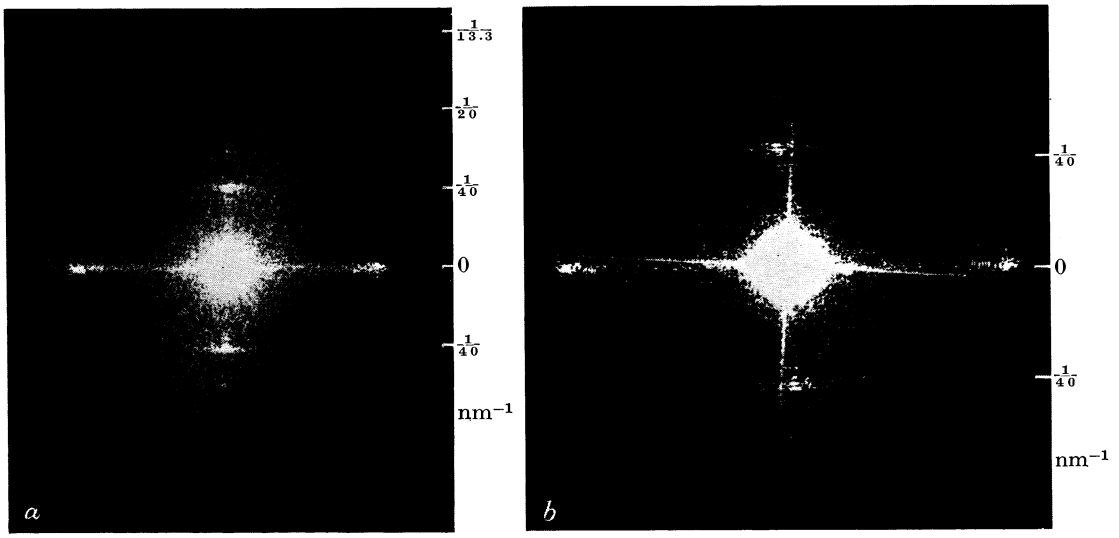

FIGURE 6. (*a*) Optical diffraction pattern obtained from the whole area of the micrograph shown in figure 5. (*b*) Pattern from a smaller area.

PHILOSOPHICAL TRANSACTIONS OF THE ROYAL SOCIETY B BIOLOGICAL SCIENCES

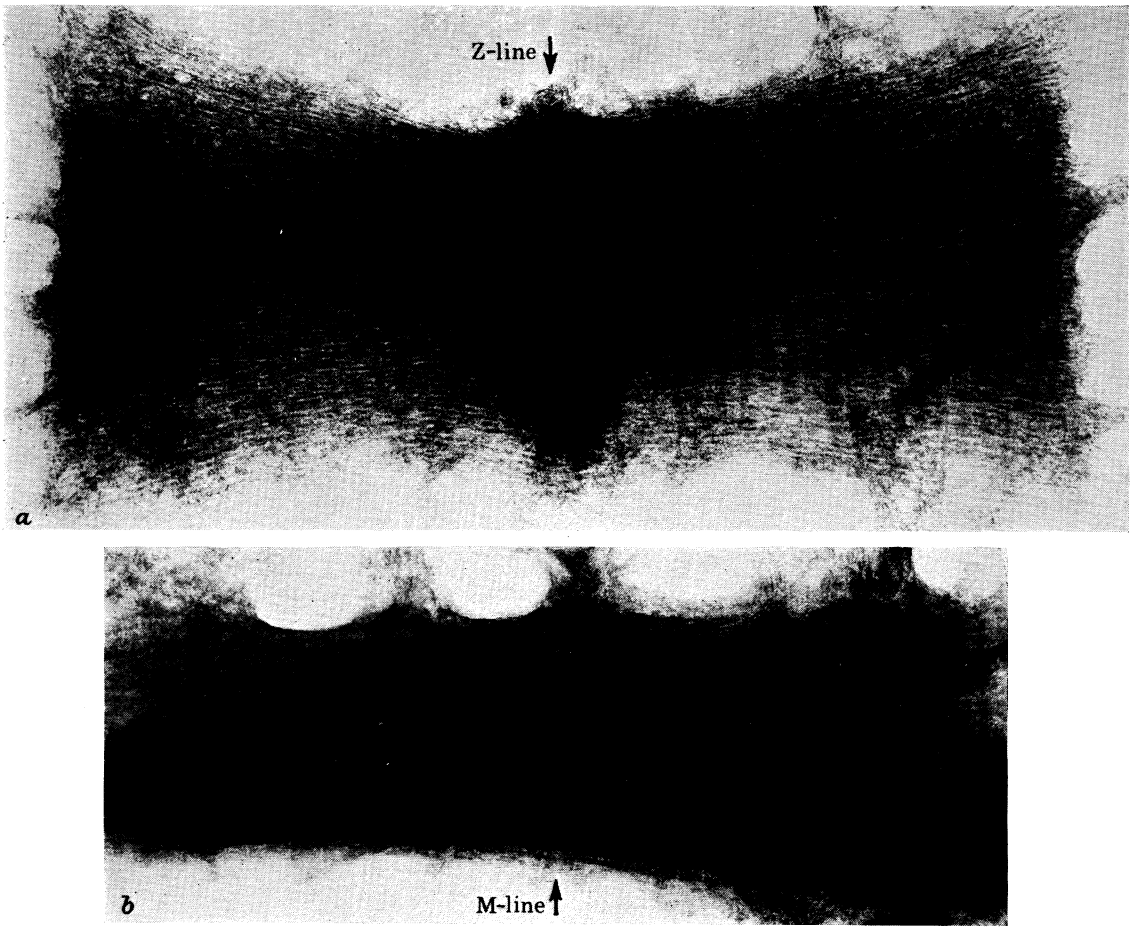

FIGURE 7. Electron micrographs of (*a*) an I segment, (*b*) an A segment, both negatively stained with 1% uranyl acetate (magn. of both ×80 000).

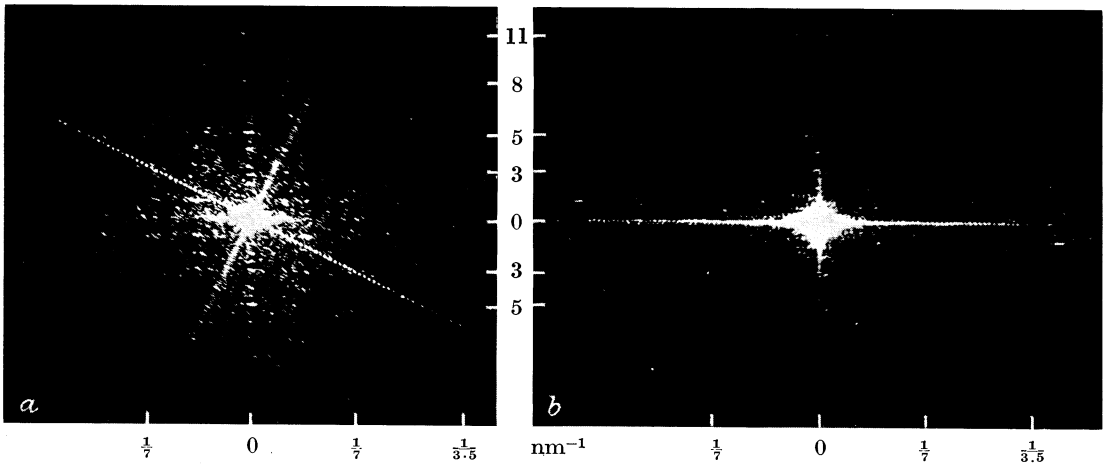

FIGURE 8. (*a*) Optical diffraction pattern recorded from one half of the A segment shown in figure 7*b*. (*b*) Pattern recorded from half of another A segment.

PHILOSOPHICAL TRANSACTIONS OF THE ROYAL SOCIETY B BIOLOGICAL SCIENCES

FIGURE 4. Impure actin paracrystals (KI method), fixed with glutaraldehyde and negatively stained with 1% potassium phosphotungstate, pH 7.0 (magn. ×230 000).

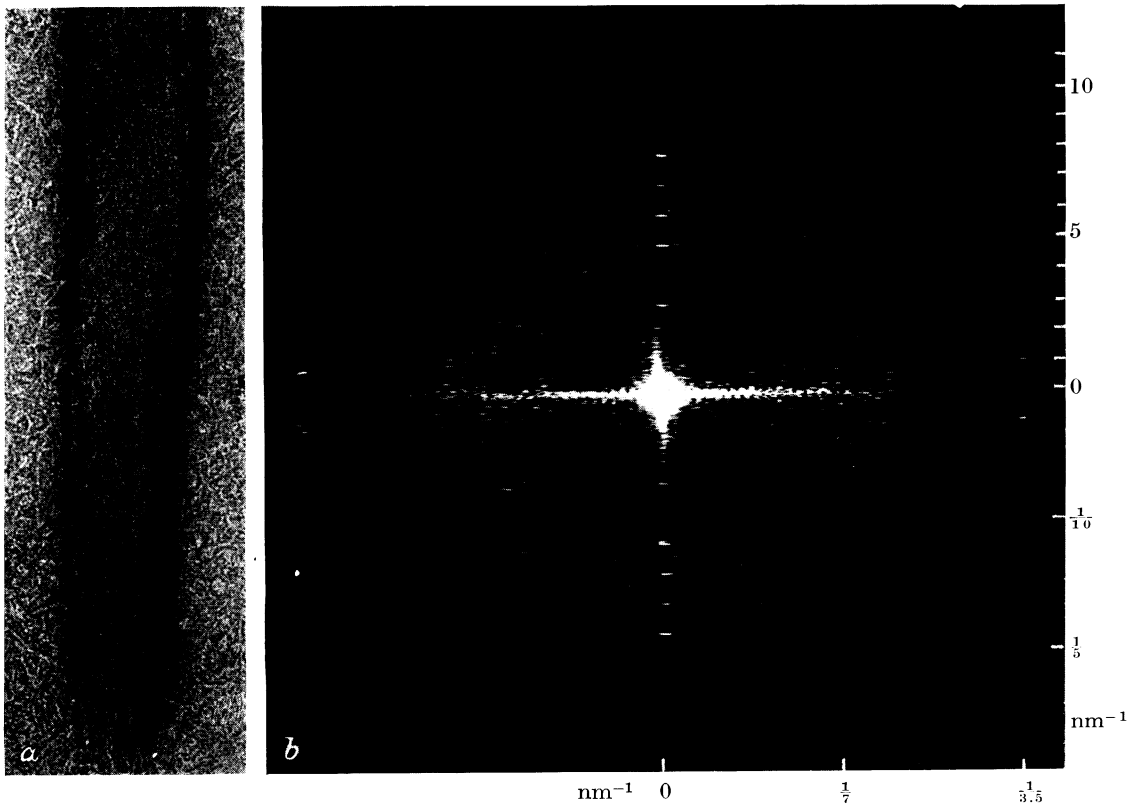

FIGURE 9. Light meromyosin paracrystal, negatively stained with 1% uranyl acetate (magn. ×90 000), and its optical diffraction pattern (from work of our colleague, Dr G. W. Offer and P. M. Bennett).

PHILOSOPHICAL TRANSACTIONS OF THE ROYAL SOCIETY B BIOLOGICAL SCIENCES

The 38.5 nm spacing (the I band spacing) and the 44.5 and 14.5 nm spacings are very similar to the spacings of certain reflexions in the meridional X-ray diffraction patterns obtained by Huxley (1967) and by Huxley & Brown (1967). These authors attribute the X-ray reflexions at 1/38.5 and 1/44.2 nm^{-1} to extra material associated with the thin and thick filaments respectively, and correlate them with the axial periodicities observed in electron micrographs of thin sections. They attribute the X-ray reflexion at 1/14.3 nm^{-1} to the subunit repeat along the myosin filament. Our results support the conclusion that the 38.5 and 44.2 nm X-ray reflexions correspond to the I and A band periodicities respectively. Moreover, we detect a reflexion corresponding to the 14.3 nm X-ray reflexion and, by careful measurement of the optical diffraction patterns, we can show that this reflexion (at 1/14.5 nm^{-1}) is *not* merely the third order of that at 1/44.5 nm^{-1}. The one spacing is consistently greater than three times the other; moreover, if these reflexions *were* the first and third orders of the same periodicity, the second order would probably be present. The presence of these two reflexions, with the correct relative spacings, in the optical diffraction patterns from the H zones, confirms the assignment of the corresponding X-ray reflexions to the A filaments. We have the advantage with optical diffraction that we can often identify in the micrograph the structural elements giving the various diffraction spectra (merely by masking out all except the region of interest).

The other meridional reflexions from the H zones, namely those with spacings 50, 18.5 (both weak) and 27 nm (medium), also correlate with meridional reflexions in the X-ray diffraction patterns from living muscle (Huxley & Brown 1967; Haselgrove 1970).

Figure 6*b* shows that the 38.5 nm, I band reflexion, which appears as a single, wide reflexion in the more heavily exposed pattern in figure 6*a*, is split into two in the meridional direction. The splitting is caused by interference between the two halves of the I band. The diffraction pattern of the two halves of the I band is the product of the diffraction pattern of one half and an interference function. The interference function is a set of fine fringes whose separation depends on the separation of the two halves. In figure 6*b* the 38.5 nm reflexion is split into two approximately equal reflexions. This shows that the Z line interpolates a distance of about $(n+\frac{1}{2}) \times 38.5$ nm between the two halves of the I band ($n = 0, 1, 2, \ldots$). The reflexion at 1/44.5 nm^{-1} is usually sharply defined in the meridional direction, with little sign of splitting.

There is other 'fine structure' in the meridional pattern. Numerous, weak, closely spaced reflexions can be seen along the meridian in figures 6*a* and 6*b*. These occur because the filaments of the sarcomere behave as diffracting units of limited length and therefore give rise to subsidiary maxima in the diffraction pattern. Similar fine structure can be observed in the high resolution X-ray diffraction patterns of Huxley & Brown (1967) and has been discussed by them. (We understand that G. Borisy & H. E. Huxley (unpublished) have also studied optical diffraction patterns of muscle sections and have obtained results similar to those discussed above.)

Some of the optical diffraction patterns show the 38.5 nm, I band reflexion extended into a layer-line, especially when long exposures are made, and the layer-line shows sampling. This implies that the stripe material is discontinuous across the I band. The electron micrographs indicate that the material is located on the filaments, rather than between them. This is in agreement with the model of actin + regulatory proteins discussed in the previous section. The layer-line at 1/38.5 nm^{-1} is not detected in the X-ray diffraction patterns of Huxley & Brown. Possibly it is present, but masked by the rather broad myosin layer-line at 1/42.4 nm^{-1} (which is not present in the optical diffraction pattern). Further along the myosin layer-line there is a diffuse reflexion of axial spacing 40 nm, but this reflexion is further away from the

meridian than the limit of the layer-line generally observed in the optical diffraction pattern (see Hanson 1968*a*, for a discussion of the origin of this 40 nm X-ray reflexion).

A segments

The assemblies of thin and thick filaments, whose structure in sectioned myofibrils was considered above, can also be examined intact in negatively stained preparations. 'I segments' and 'A segments' can be prepared from myofibrils when these are mechanically disintegrated while maintained in a relaxed state. The I segment, which consists of the Z disk with its two attached sets of thin filaments, was first described by Huxley (1963). I segments appear striped (figure 7*a*, plate 38). Optical diffraction patterns obtained from them are similar to those from actin paracrystals, but less well defined. The A segment is the set of thick, A band filaments from which the thin filaments have been withdrawn (J. Hanson, unpublished). It shows a bipolar band pattern (figure 7*b*). The central L region consists of the M line flanked by the two stain-filled zones where the filaments lack projections. On either side of the L region there are ten main, transverse bands, each containing a pattern of subsidiary bands.

The diffraction pattern shown in figure 8*a*, plate 38, was recorded from one half of the A segment shown in figure 7*b*. A series of meridional reflexions, of periodicity approximately 1/43 nm^{-1}, extends to the eleventh order. Of the higher orders, the fifth, eighth and eleventh are strong compared with others in the higher angle region. We note that the eighth and eleventh orders are relatively strong in the meridional X-ray diffraction patterns recorded from living muscle by Huxley & Brown (1967). Figure 8*a* also shows equatorial reflexions. Of particular interest are the reflexions occurring at 1/7 and 1/3.5 nm^{-1}. The spacings of these reflexions are commensurate with the distances expected between molecules or small groups of molecules. A reflexion near 1/3.5 nm^{-1} can be seen more clearly in figure 8*b*, recorded from another A segment. It is off-equatorial, suggesting that the molecules in the filaments are inclined slightly to the filament axis. Similar off-equatorial reflexions can be seen in figure 9*b*, plate 39, which was obtained from an electron micrograph of a paracrystal of light meromyosin (figure 9*a*). Here too, the eighth and eleventh orders of a meridional repeat of about 43 nm are relatively strong. These common features in the diffraction patterns indicate that the electron micrographs of the A segments give information on the arrangement of the light meromyosin in the shaft of the myosin filament. The projections (heavy meromyosin) are presumably too disorganized to be revealed since there is little in the off-meridional diffraction that resembles the myosin layer-lines in the X-ray diffraction patterns. Similarly, the projections generally appear disorganized in electron micrographs of single thick filaments, both natural and self-assembled from myosin. Further study of A segments and of single filaments should provide a more detailed model of the molecular packing.

Figure 9 is a good example of the power of optical diffraction to reveal well defined periodicities when the micrograph itself appears confused, little different from the background. The diffraction pattern is *not* of the background!

Concluding remarks

We have considered several examples of the different kinds of specimen that can be prepared from muscles for examination by electron microscopy: thin sections of the intact contractile

apparatus, filament arrays separated from it, and paracrystalline structures assembled *in vitro* from selected molecular components of the filaments. The micrographs of all these different specimens contain information about their periodic structure, and the optical diffraction technique provides a powerful method for analysing and comparing quantitatively this information. Furthermore, optical diffraction can help to interpret the detailed X-ray diffraction patterns from living muscle that are now available. Thus X-ray diffraction and electron microscopy are made more effectively complementary to one another.

We are indebted to Mr Z. Gabor for expert photographic assistance. We thank our colleagues Drs A. Elliott, G. W. Offer and E. M. Rome for discussion.

Appendix. Preparative methods

(*a*) *Actin paracrystals*

F actin, prepared by the Straub method, was purified in two ways. One was based on the work of Martonosi (1962), who showed that the polymer formed in 0.6 mmol l^{-1} $MgCl_2$ is free of other proteins. The other purification method involved gel filtration (Rees & Young 1967).

Two kinds of impure actin were used. One was prepared by the KI extraction method of Szent-Györgyi (1951); the F actin was collected by centrifugation and was resuspended in 0.1 mol l^{-1} KCl. The other kind of impure actin was made by mixing purified F actin, in 0.1 mol l^{-1} KCl, with incompletely purified tropomyosin. The tropomyosin was prepared by the method of Müeller (1966), but purification was stopped after only one isoelectric precipitation and one ammonium sulphate precipitation.

Paracrystals were formed by dialysis against 0.1 mol l^{-1} $MgCl_2$ buffered with 5 mmol l^{-1} histidine-HCl at pH 6.6.

(*b*) *A and I segments*

The thigh muscles of a frog (*Rana temporaria*) were excised into cold calcium-chelating solution (100 mmol l^{-1} KCl, 2 mmol l^{-1} EGTA,† 2 mmol l^{-1} $MgCl_2$, buffered with 67 mmol l^{-1} phosphate at pH 7.0), placed in the cold room for 1 h, and then disintegrated into myofibrils. These were collected by centrifugation and resuspended in the above solution, with the addition of 2 mmol l^{-1} ATP to relax the fibrils. After about 15 min on ice, further blending released A and I segments as well as single filaments. A Virtis homogenizer with a 10 ml flask was used.

(*c*) *Electron microscope preparations*

Routine negative contrast methods were generally used. However, special techniques were necessary for impure actin paracrystals and A segments.

(i) The stripes in the impure actin paracrystals were only observed when the paracrystals had been fixed with 1 % glutaraldehyde, unbuffered, in 0.1 mol l^{-1} $MgCl_2$. (Note that fixation did not affect the structure of pure actin paracrystals.)

(ii) The structure of the A segments was seen most clearly when the preparation had been rinsed with 0.1 mol l^{-1} ammonium acetate before uranyl acetate was applied.

† EGTA: ethylene glycol bis-(β-aminoethyl ether)-*N*,*N*′-tetra-acetate.

PHILOSOPHICAL TRANSACTIONS OF THE ROYAL SOCIETY B BIOLOGICAL SCIENCES

References (O'Brien *et al.*)

Ebashi, S. & Endo, M. 1968 *Prog. biophys. molec. Biol.* **18**, 123.
Ebashi, S., Endo, M. & Ohtsuki, I. 1969 *Q. Rev. Biophys.* **2**, 351.
Hanson, J. 1967 *Nature, Lond.* **213**, 353.
Hanson, J. 1968*a* *Q. Rev. Biophys.* **1**, 177.
Hanson, J. 1968*b* In *Symposium on muscle* (eds. E. Ernst and F. B. Straub), p. 93. Budapest: Akademiai Kiadó.
Hanson, J. & Lowy, J. 1963 *J. molec. Biol.* **6**, 46.
Haselgrove, J. C. 1970 Ph.D. Thesis, University of Cambridge.
Huxley, H. E. 1963 *J. molec. Biol.* **7**, 281.
Huxley, H. E. 1967 *J. gen. Physiol.* **50**, 71.
Huxley, H. E. & Brown, W. 1967 *J. molec. Biol.* **30**, 383.
Klug, A. & DeRosier, D. J. 1966 *Nature, Lond.* **212**, 29.
Klug, A. & Franklin, R. E. 1958 *Discuss. Faraday Soc.* **25**, 104.
Lowy, J. & Vibert, P. J. 1967 *Nature, Lond.* **215**, 1254.
Martonosi, A. 1962 *J. biol. Chem.* **237**, 2795.
Marvin, D. A. 1958 *Discuss. Faraday Soc.* **25**, 203.
Marvin, D. A., Spencer, M., Wilkins, M. H. F. & Hamilton, L. D. 1961 *J. molec. Biol.* **3**, 547.
Müeller, H. 1966 *Biochem. Z.* **345**, 300.
Page, S. G. 1964 *Proc. Roy. Soc. Lond.* B **160**, 460.
Page, S. G. & Huxley, H. E. 1963 *J. Cell Biol.* **19**, 369.
Rees, M. K. & Young, M. 1967 *J. Biol. Chem.* **242**, 4449.
Schaub, M. C. & Perry, S. V. 1969 *Biochem. J.* **115**, 993.
Selby, C. C. & Bear, R. S. 1956 *J. biophys. biochem. Cytol.* **2**, 71.
Szent-Györgyi, A. G. 1951 *J. biol. Chem.* **192**, 361.
Taylor, C. A. & Lipson, H. 1964 *Optical transforms*. London: G. Bell and Sons Ltd.

PHILOSOPHICAL TRANSACTIONS OF THE ROYAL SOCIETY B BIOLOGICAL SCIENCES

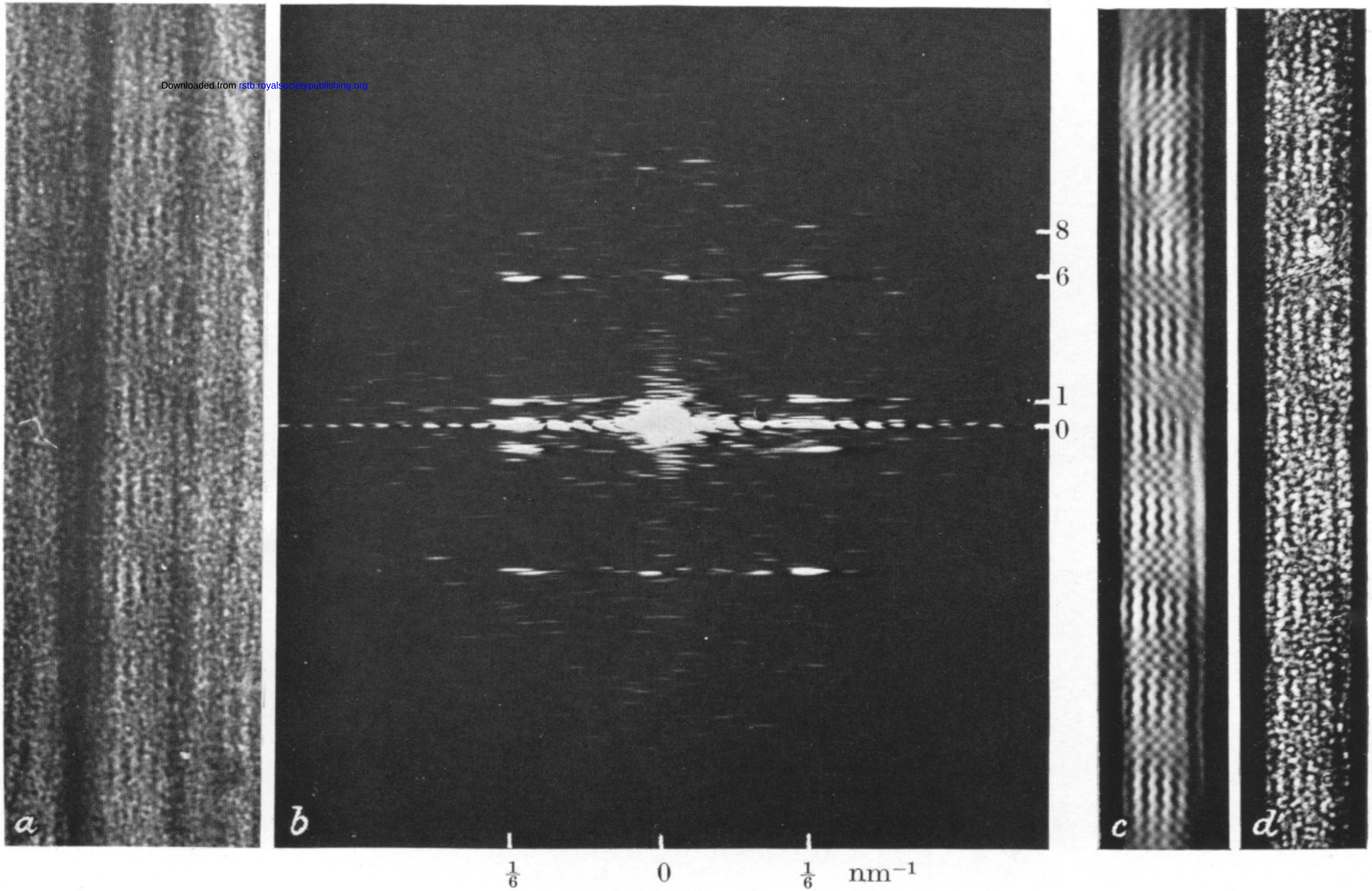

FIGURE 1. (*a*) A paracrystal of highly purified actin, negatively stained with 1% uranyl acetate. (*b*) Optical diffraction pattern of part of (*a*). (*c*) Filtered image of part of (*a*). The filter masked out all but the strong diffracted rays and hence excluded the 'noise' spectra, that is, the diffracted rays that could not be indexed on the actin lattice. (*d*) The image of the same part of (*a*) recorded by the apparatus without a filter. (Magnification of (*a*), (*c*) and (*d*) $\times 270\,000$.) The protein is white in (*a*), (*c*) and (*d*).

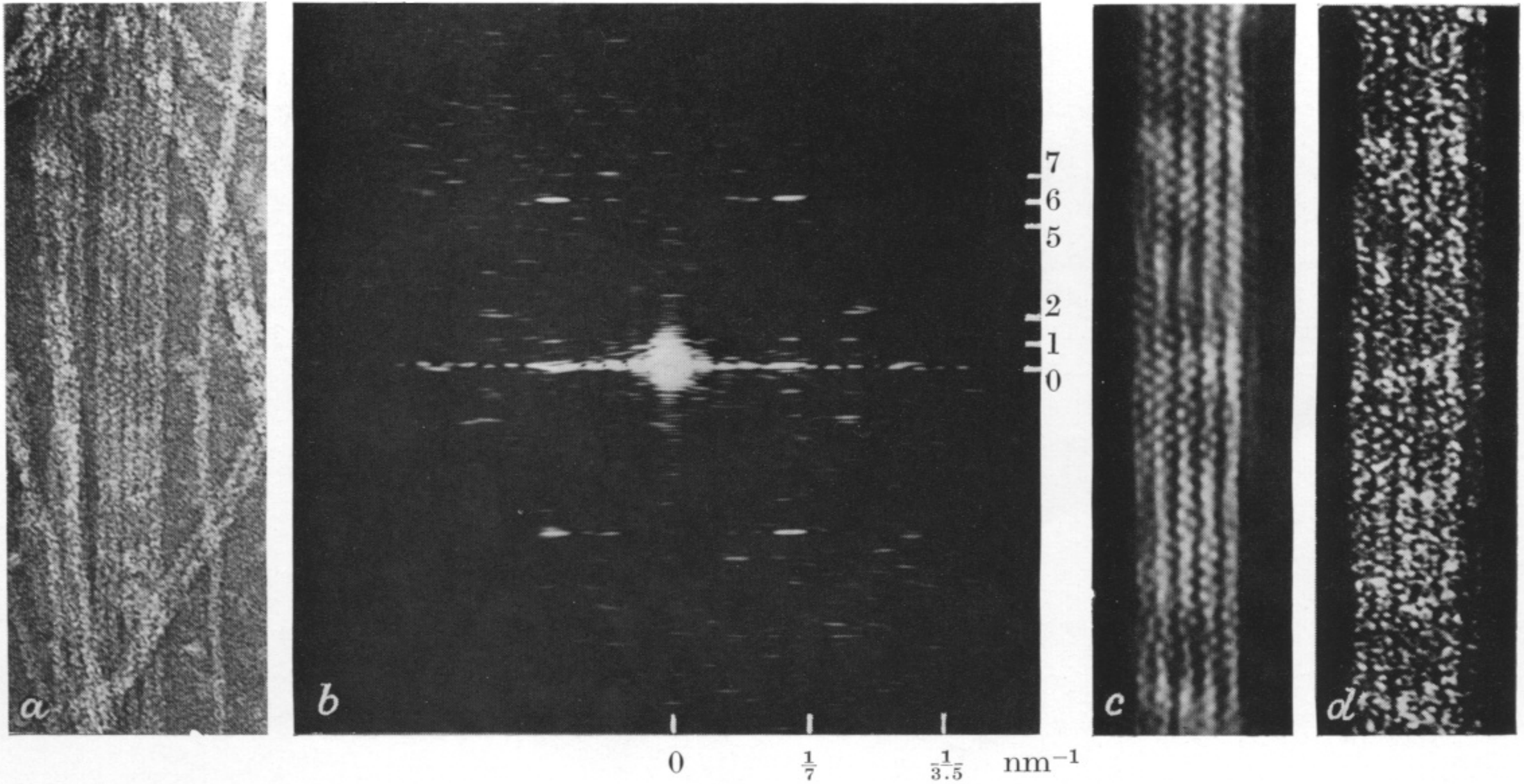

FIGURE 3. (*a*) to (*d*) The sequence of figure 1 repeated for an impure actin paracrystal (pure actin plus impure tropomyosin). The preparation was fixed with glutaraldehyde and negatively stained with 1% uranyl acetate. The optical diffraction pattern differs from that in figure 1 chiefly in the change of row-line spacing, reversal of relative intensities of the first and second layer-lines, and introduction of weak row-lines midway between the main ones. In the filtered image, the cross-over points may be seen more clearly near the centre of the photograph, especially when it is viewed obliquely along its length. (Magnification of (*a*) $\times 160\,000$, (*c*) and (*d*) $\times 270\,000$.)

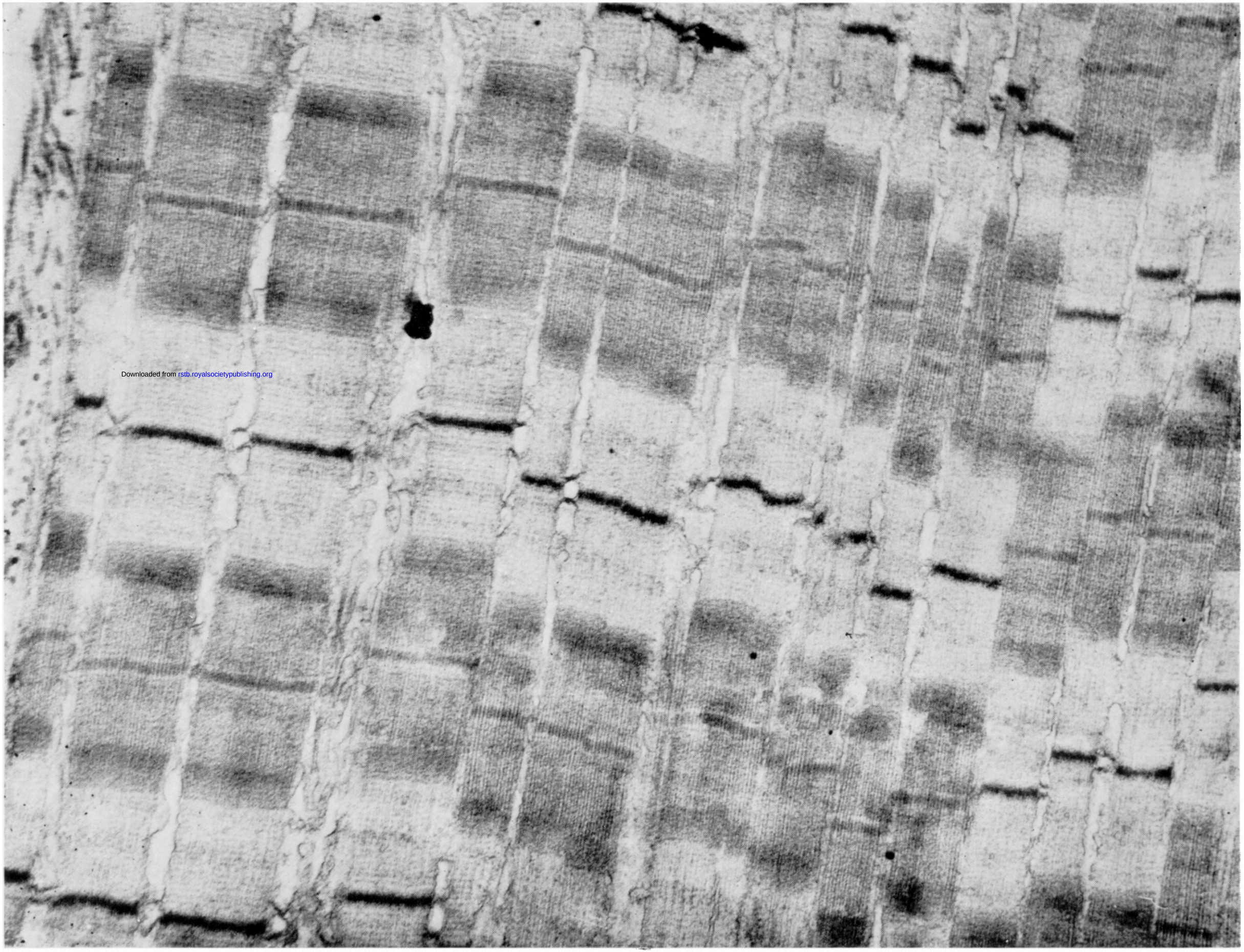

FIGURE 5. Longitudinal section of frog sartorius muscle, positively stained with phosphotungstic acid. The muscle was clamped at either end during fixation with OsO_4 and dehydration with ethanol, and was electrically stimulated during fixation. Changes of filament length were thus minimized (Page 1964; Page & Huxley 1963). The section was cut with the knife edge parallel to the fibre axis (magn. $\times 24\,000$).

PHILOSOPHICAL TRANSACTIONS OF THE ROYAL SOCIETY B BIOLOGICAL SCIENCES

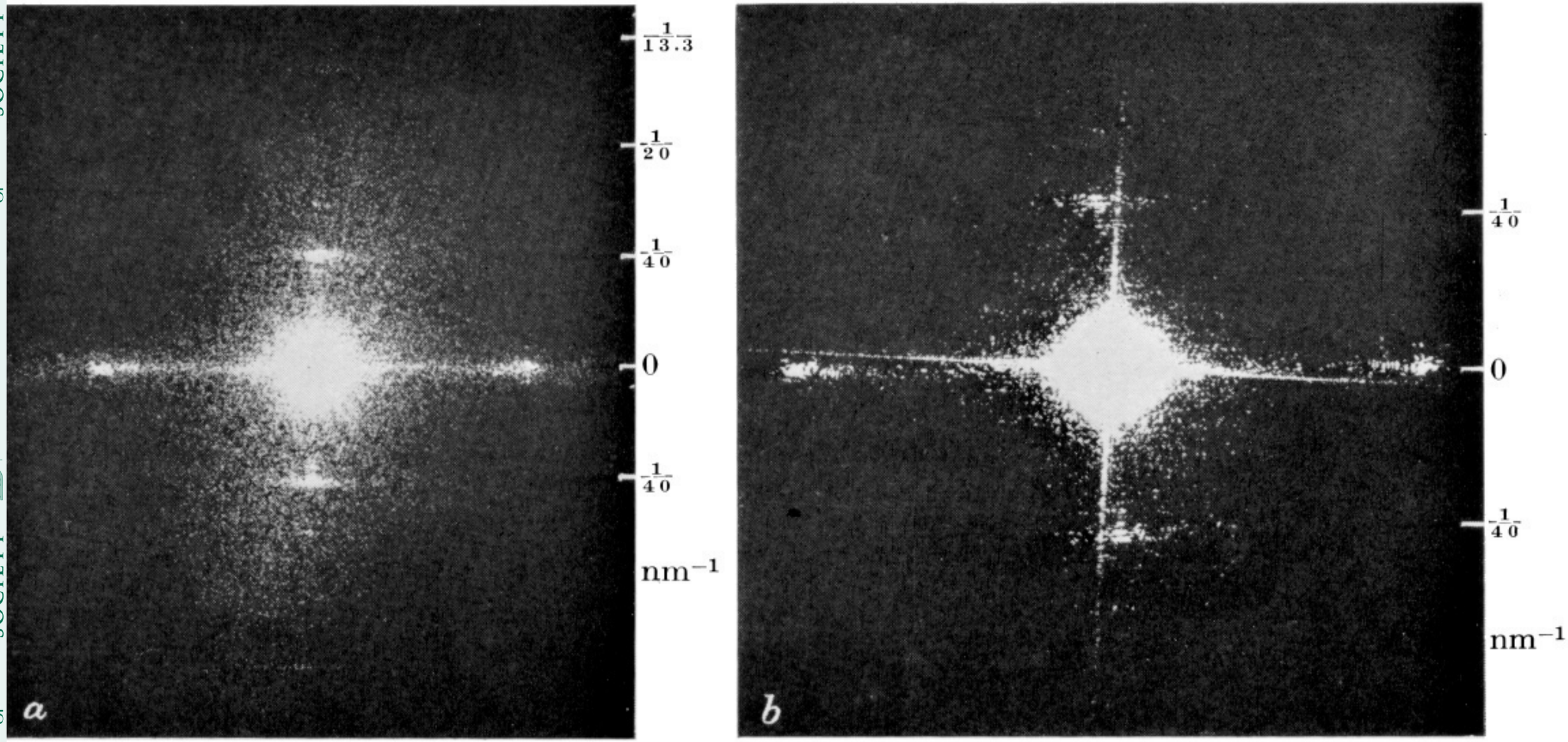

FIGURE 6. (*a*) Optical diffraction pattern obtained from the whole area of the micrograph shown in figure 5. (*b*) Pattern from a smaller area.

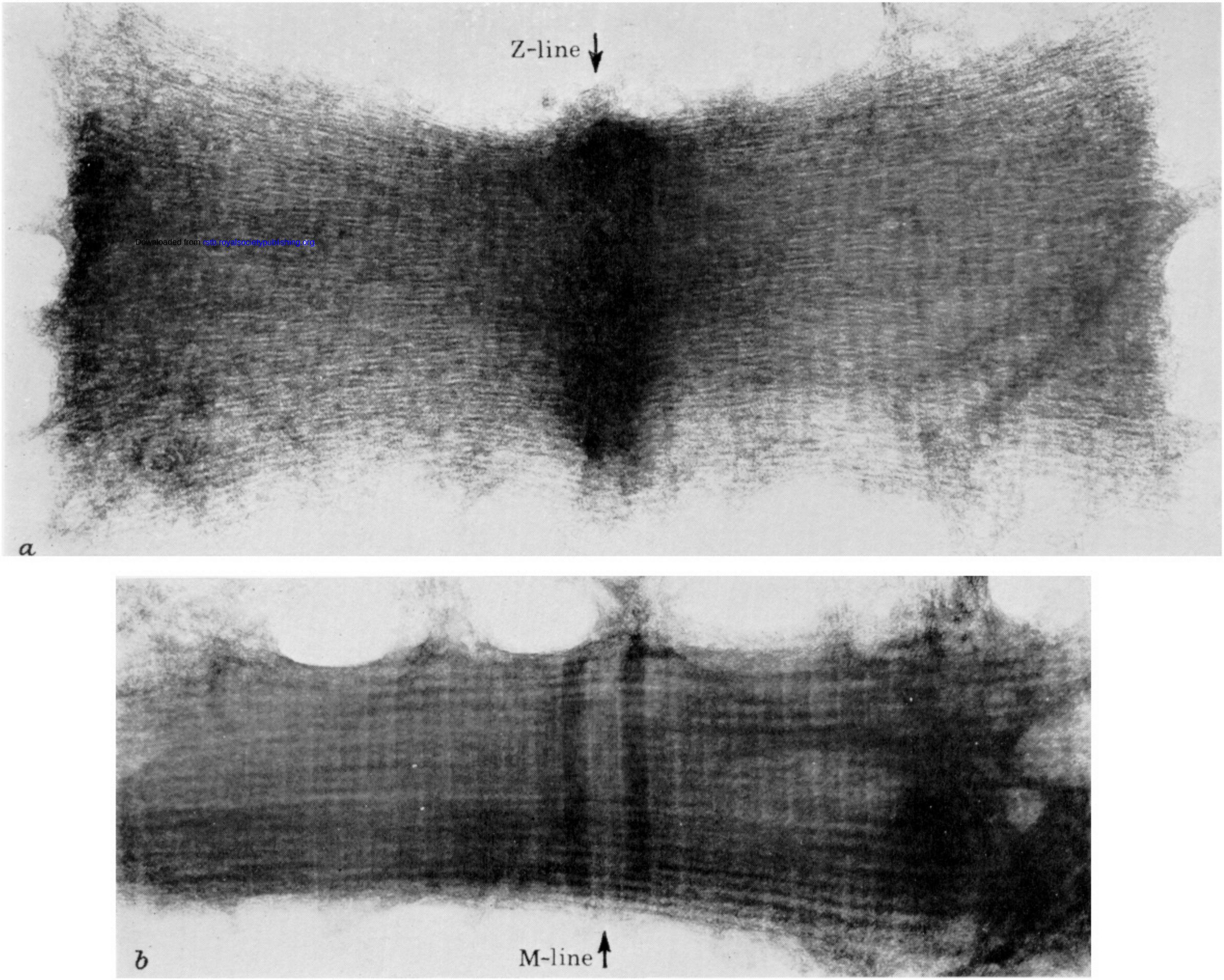

FIGURE 7. Electron micrographs of (*a*) an I segment, (*b*) an A segment, both negatively stained with 1% uranyl acetate (magn. of both × 80 000).

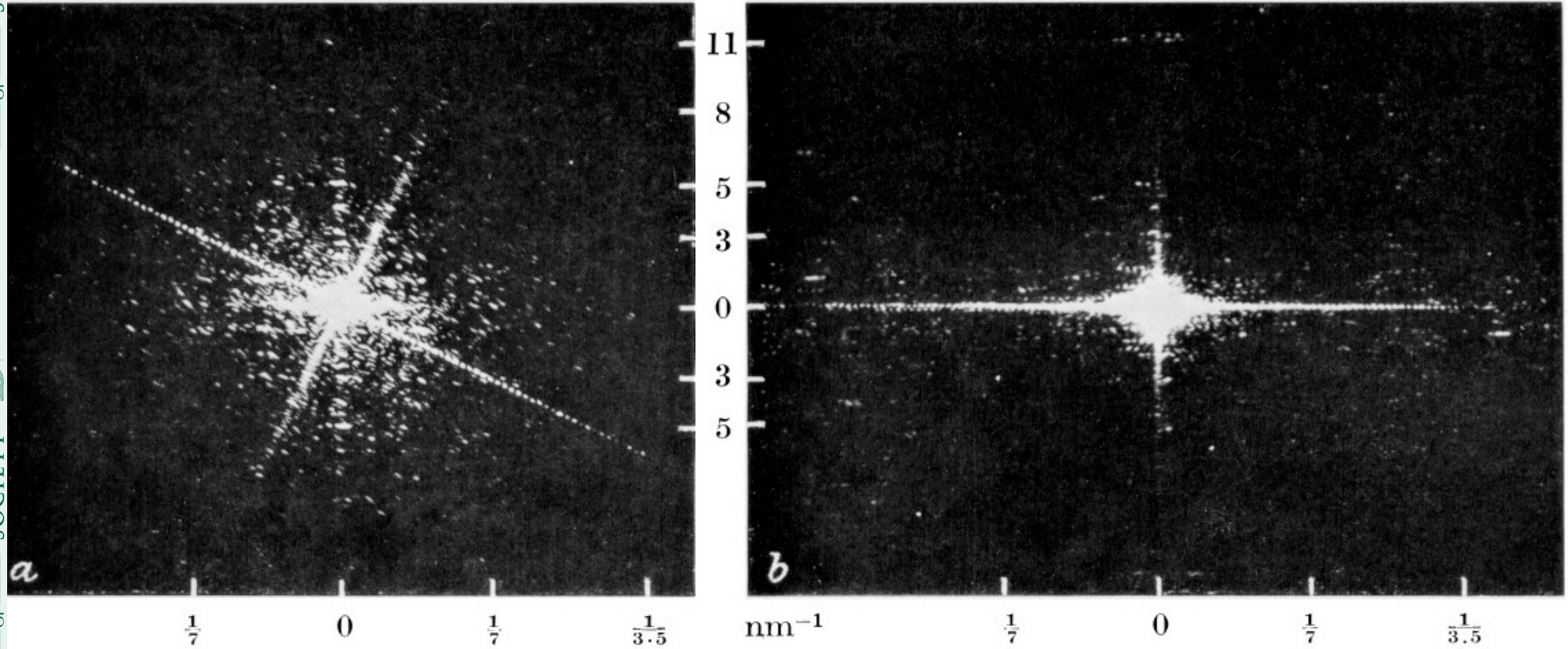

FIGURE 8. (*a*) Optical diffraction pattern recorded from one half of the A segment shown in figure 7*b*. (*b*) Pattern recorded from half of another A segment.

PHILOSOPHICAL TRANSACTIONS OF THE ROYAL SOCIETY B BIOLOGICAL SCIENCES

FIGURE 4. Impure actin paracrystals (KI method), fixed with glutaraldehyde and negatively stained with 1% potassium phosphotungstate, pH 7.0 (magn. ×230 000).

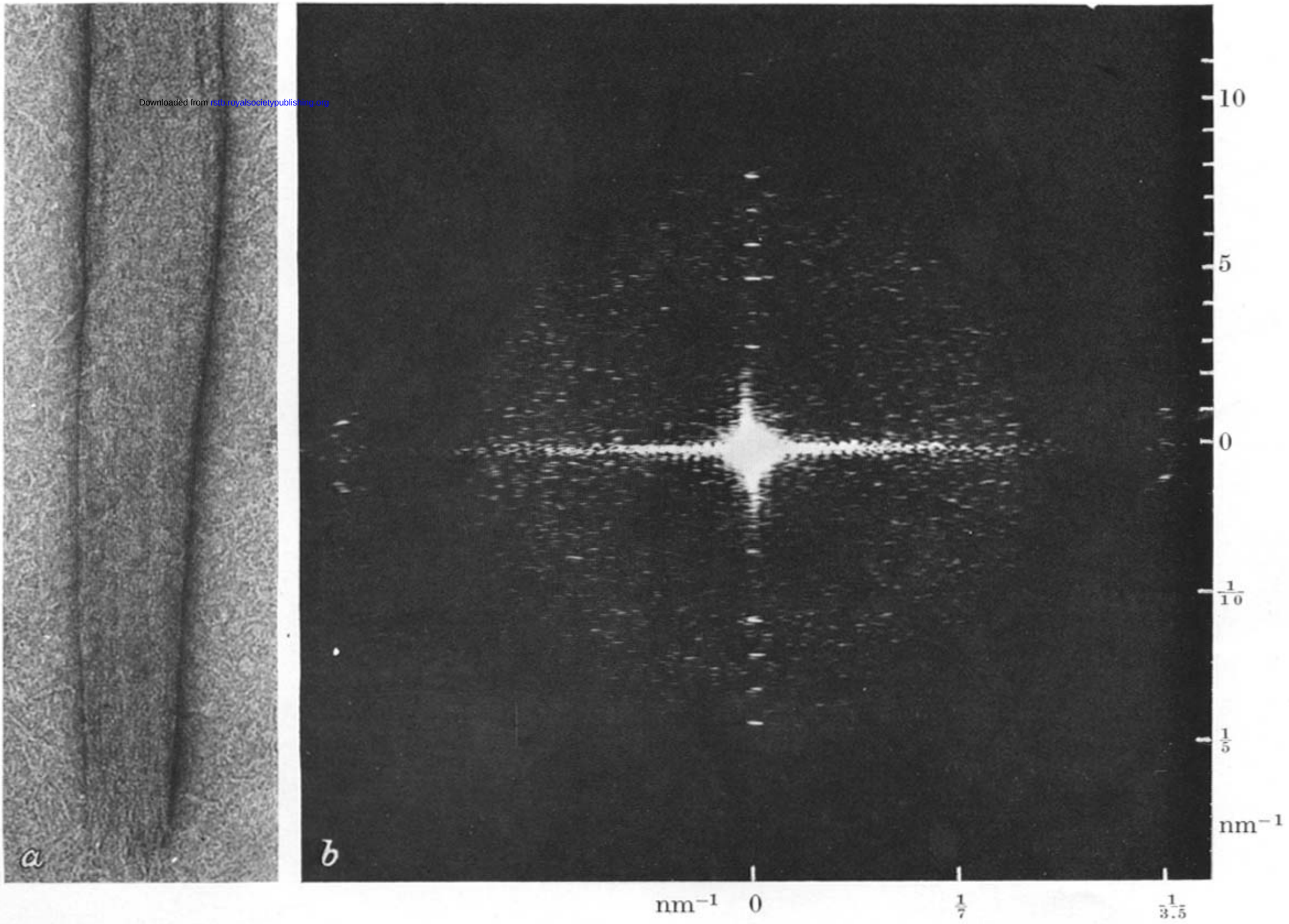

FIGURE 9. Light meromyosin paracrystal, negatively stained with 1% uranyl acetate (magn. ×90 000), and its optical diffraction pattern (from work of our colleague, Dr G. W. Offer and P. M. Bennett).